Journal of Solid State Chemistry **166,** 305–310 (2002)
doi:10.1006/jssc.2002.9591

X-Ray Single-Crystal Studies of ZrRhGa, HfRhGa, and $ZrRh_{0.710(4)}In$

Markus F. Zumdick

Fraunhofer Institut für Fertigungstechnik und Materialforschung, Winterbergstrasse 28, 01277 Dresden, Germany and Institut für Anorganische und Analytische Chemie, Universität Münster, Wilhelm-Klemm-Strasse 8, D-48149 Münster, Germany

Rainer Pöttgen[1]

Institut für Anorganische und Analytische Chemie, Universität Münster, Wilhelm-Klemm-Strasse 8, D-48149 Münster, Germany

Vasyl' I. Zaremba

Inorganic Chemistry Department, Ivan Franko Lviv National University, Kyryla and Mephodiya Street 6, 79005 Lviv, Ukraine

and

Rolf-Dieter Hoffmann

Institut für Anorganische und Analytische Chemie, Universität Münster, Wilhelm-Klemm-Strasse 8, D-48149 Münster, Germany

Received December 26, 2001; in revised form March 5, 2002; accepted March 15, 2002

ZrRhGa, HfRhGa, and $ZrRh_{0.710(4)}In$ were prepared by arc melting of the elements under an argon atmosphere and subsequent annealing. The three compounds were investigated by X-ray diffraction on powders and single crystals: ZrNiAl-type, space group $P\bar{6}2m$, $a = 721.4(2)$ pm, $c = 336.7(2)$ pm, $wR2 = 0.0366$, 191 F^2 values, 14 parameters for ZrRhGa, $a = 724.2(3)$ pm, $c = 328.0(1)$ pm, $wR2 = 0.0326$, 191 F^2 values, 14 parameters for HfRhGa, and $a = 741.91(7)$ pm, $c = 335.8(1)$ pm, $wR2 = 0.0339$, 202 F^2 values, and 14 parameters for $ZrRh_{0.710(4)}In$. Anisotropic refinement of the Rh1 positions of ZrRhGa and HfRhGa showed extremely large U_{33} values. These sites have been refined with a split position 00z (2*e*) instead of 000 (2*a*) with an occupancy of 50%. Both gallides have carefully been investigated by low-temperature X-ray data and electron diffraction. These data gave no indication for an ordering of the rhodium atoms. Structural motifs of both gallides are rhodium-centered trigonal prisms [$Rh1Ga_6$], [$Rh2Zr_6$], and [$Rh2Hf_6$], respectively. The prisms are condensed via common edges and faces. The Rh1 position in the indide is occupied only by 12% resulting in the composition $ZrRh_{0.710(4)}In$ for the investigated crystal. The geometrical restrictions and chemical bonding of these intermetallics are discussed.

Key Words: **metal-rich compounds; crystal structure; gallium; indium.**

INTRODUCTION

Recently, we reported on the formation of a new superstructure (1, 2) of the ZrNiAl type (2–4) which itself is an ordered variant of the well-known Fe_2P structure. The formation of this peculiar superstructure was first observed for HfRhSn (1) and it is most likely due to a puckering effect. The HfRhSn structure has two crystallographically independent rhodium sites with a trigonal prismatic coordination, i.e. [$Rh1Hf_6$] and [$Rh2Sn_6$]. In the superstructure the hafnium prisms show a strong distortion and displacement of the rhodium atoms, leading to a doubling of the c lattice parameter. The formation of the superstructure seems to depend on the c/a ratio and it occurs below $c/a \approx 0.5$ for the subcell. So far, this superstructure was clearly resolved for ScPtSn (5), ZrPtGa, ZrRhSn (2), ZrIrSn, HfCoSn, and HfRhSn (1) on the basis of single-crystal X-ray data. All these compounds show c/a ratios smaller than 0.5. When the c/a ratio is close to 0.5, the distortions are not very pronounced. In the case of ZrNiAl

[1]To whom correspondence should be addressed. Fax: +49-251-83-36002. E-mail: pottgen@uni-muenster.de.

0022-4596/02 $35.00

(2), α-YbPdSn (6), and YbPtSn (7), the transition metal atoms within the trigonal zirconium or ytterbium prisms showed only a larger U_{33} displacement parameter. No superstructure reflections could be detected.

The so far smallest c/a ratio of 0.421 within the family of Fe_2P-related intermetallics was recently observed for $Ti_3Rh_2In_3$ (8). Due to the small titanium atoms, the unit cell considerably contracts. This way the trigonal indium prisms around the origin become very small and consequently we found no rhodium occupancy in these prisms. We can thus formally write $Ti_3Rh_2\square In_3$ in emphasizing the void at the origin.

In this context, we were interested in the precise crystal structures of those Fe_2P-related intermetallics with a c/a ratio significantly smaller than 0.5. The gallides ZrRhGa (c/a = 0.467) and HfRhGa (c/a = 0.453) (9) have already been reported many years ago; however, only on the basis of X-ray powder data. Herein, we report on the structure refinements of ZrRhGa and HfRhGa based on single-crystal X-ray data which clearly resolved a split position for the rhodium atoms at the origin. Furthermore, we prepared $ZrRh_{0.710(4)}In$ the first compound in the zirconium–rhodium–indium system. For $ZrRh_{0.710(4)}In$, we observed only an occupancy of 12% rhodium in the void at the origin.

EXPERIMENTAL

Starting materials for the synthesis of ZrRhGa, HfRhGa, and $ZrRh_{0.710(4)}In$ were zirconium pieces (Johnson-Matthey, >99.5%), hafnium turnings (Heraeus, >99.9%), rhodium powder (Degussa-Hüls, 200 mesh, >99.9%), gallium pieces (Wacker, >99.9%) and indium tear drops (Johnson Matthey, >99.9%). In a first step, the small zirconium (hafnium) pieces were arc-melted to buttons under argon in a miniaturized arc melting apparatus (10). The argon was purified before over titanium sponge (900 K), silica gel, and molecular sieves. This pre-melting procedure strongly reduces a shattering of these elements during the exothermic reactions. The rhodium powder was pressed to small pellets (6 mm diameter). The zirconium (hafnium) buttons and the rhodium pellets were then mixed in the ideal 1:1:1 atomic ratio and melted to buttons in the arc furnace under an argon pressure of about 600 mbar. The melted ingots were turned over and remelted three times on each side to ensure homogeneity. The total weight losses were always smaller than 0.5%. The silvery products ZrRhGa, HfRhGa, and $ZrRh_{0.710(4)}In$ were extremely brittle and well crystallized. The polycrystalline samples are stable in moist air over a period of several months. No deterioration could be observed. Powders are dark gray. The crystals of the gallides were irregularly shaped, while $ZrRh_{0.710(4)}In$ forms small needles.

In order to investigate the possibility of a superstructure formation (see discussion below), the samples of ZrRhGa and HfRhGa were annealed at different temperatures after the arc-melting procedure. The samples were therefore sealed in evacuated silica tubes and annealed in a resistance furnace. Various parts of the arc-melted buttons were annealed at 1170, 970, and 770 K, respectively, for periods of 2 weeks. None of the powder patterns, however, showed additional reflections in the X-ray powder diagrams.

The $ZrRh_{0.710(4)}In$ sample was analyzed by EDX measurements using a LEICA 420 I scanning electron microscope with elemental zirconium, rhodium, and indium arsenide as standards. No impurity elements were detected and the analyses (37 ± 1 at% Zr: 25 ± 1 at% Rh: 38 ± 1 at% In) of several single crystals were in good agreement with the ideal composition 36.9 at% Zr: 26.2 at% Rh: 36.9 at% In, i.e., $ZrRh_{0.710(4)}In$. The standard deviations account for the various analyses obtained for different crystallites.

All samples were characterized through Guinier powder patterns which were recorded with Cu$K\alpha_1$ radiation using α-quartz (a = 491.30 pm, c = 540.46 pm) as an internal standard. The patterns could completely be indexed with hexagonal cells. The lattice parameters (see Table 1) were obtained from least-squares fits of the Guinier data. To assure correct indexing, the observed patterns were compared with calculated ones (11) taking the atomic positions from the structure refinements. The lattice parameters obtained from the single crystals were in accordance with the powder data. For ZrRhGa and HfRhGa we observed good agreement with the previously published X-ray powder data by Dwight (9): a = 720.7 pm, c = 336.6 pm for ZrRhGa and a = 723.7, c = 329.6 pm for HfRhGa.

Single-crystal intensity data were collected at room temperature by use of a four-circle diffractometer (CAD4) with graphite monochromatized Mo$K\alpha$ (71.073 pm) radiation and a scintillation counter with pulse height discrimination. The scans were taken in the $\omega/2\theta$ mode and empirical absorption corrections were applied on the basis of psi-scan data. All relevant details concerning the data collections are listed in Table 1. The ZrRhGa crystal was additionally studied at lower temperatures (200 and 250 K) using a Stoe image plate system in oscillation mode with Mo$K\alpha$ (71.073 pm) radiation. The temperature was controlled by an OXFORD CRYOSTREAM system.

RESULTS AND DISCUSSION

Structure Refinements

Irregularly shaped single crystals of ZrRhGa and HfRhGa and a small needle of $ZrRh_{0.710(4)}In$ were isolated from the annealed samples and examined by use of a

TABLE 1
Crystal Data and Structure Refinement for ZrRhGa, HfRhGa, and $ZrRh_{0.710(4)}In$ (Space Group $P\bar{6}2m$; $Z = 3$)

Empirical formula	ZrRhGa	HfRhGa	$ZrRh_{0.710(4)}In$
Molar mass (g/mol)	263.85	351.12	308.95
Pearson symbol	*hP9*	*hP9*	*hP8.13*
Unit-cell dimensions	$a = 721.4(2)$ pm	$a = 724.2(3)$ pm	$a = 741.91(7)$ pm
(Guinier powder data)	$c = 336.7(2)$ pm	$c = 328.0(1)$ pm	$c = 335.8(1)$ pm
	$V = 0.1518\,nm^3$	$V = 0.1490\,nm^3$	$V = 0.1601\,nm^3$
Calculated density (g/cm^3)	8.66	11.74	9.62
Crystal size (μm^3)	$10 \times 20 \times 50$	$20 \times 20 \times 40$	$20 \times 20 \times 70$
Transmission ratio (max/min)	1.73	1.86	1.09
Absorption coefficient (mm^{-1})	25.8	73.3	22.7
$F(0\,0\,0)$	348	444	402
θ range for data collection	3–30°	3–30°	3–30°
Range in *hkl*	±10, ±10, ±4	±10, ±10, ±4	±10, ±10, +4
Total no. of reflections	1071	1084	1049
Independent reflections	191 ($R_{int} = 0.0652$)	191 ($R_{int} = 0.0427$)	202 ($R_{int} = 0.0603$)
Reflections with $I > 2\sigma(I)$	180 ($R_{sigma} = 0.0384$)	189 ($R_{sigma} = 0.0214$)	182 ($R_{sigma} = 0.0385$)
Data/restraints/parameters	191/0/14	191/0/14	202/0/14
Goodness of fit on F^2	1.102	1.234	1.078
Final *R* indices [$I > 2\sigma(I)$]	$R1 = 0.0201$	$R1 = 0.0140$	$R1 = 0.0202$
	$wR2 = 0.0349$	$wR2 = 0.0325$	$wR2 = 0.0323$
R indices (all data)	$R1 = 0.0270$	$R1 = 0.0143$	$R1 = 0.0279$
	$wR2 = 0.0366$	$wR2 = 0.0326$	$wR2 = 0.0339$
Flack parameter	0.02(4)	−0.01(2)	0.02(13)
Extinction coefficient	0.006(2)	0.0110(6)	0.019(2)
Largest diff. peak and hole	1.09 and $-0.91\,e/Å^3$	1.51 and $-1.09\,e/Å^3$	1.10 and $-1.03\,e/Å^3$

Buerger camera. The precession photographs showed hexagonal cells and no systematic extinctions. The noncentrosymmetric space group $P\bar{6}2m$ was found to be correct for all three structures. Further crystallographic details are listed in Table 1.

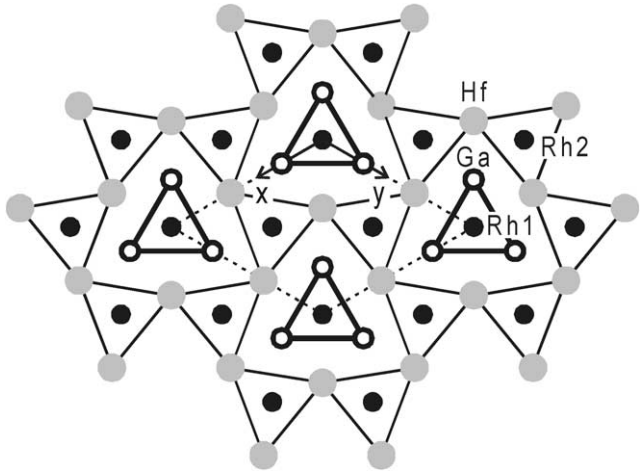

FIG. 1. Projection of the HfRhGa structure onto the *xy* plane. Hafnium, rhodium, and gallium atoms are drawn as gray, black filled, and black open circles, respectively. The trigonal prisms around the rhodium atoms are emphasized. Most atoms lie on mirror planes at $z = 0$ (thin lines) and $z = 1/2$ (thick lines). The Rh1 atoms show a split position $00z$ ($z = 0.9414$).

The starting atomic parameters were deduced from automatic interpretations of direct methods using SHELXS-97 (12) and the structures were refined using SHELXL-97 (13) (full-matrix least squares on F^2). Refinement with anisotropic displacement parameters showed extremely large U_{33} values for the Rh1 positions in ZrRhGa and HfRhGa, indicating that these atoms show a dislocation from the origin. We subsequently introduced split positions with an occupancy of 50%, i.e., Wyckoff position 2*e* $00z$ instead of 1*a* 000. These positions were then refined with isotropic displacement parameters and the refinements readily converged to low residuals (Table 1).

From direct methods, we obtained only three positions for the indide. These were identical with those obtained recently for $Ti_3Rh_2In_3$ (8), leading to the composition $Zr_3Rh_2In_3$. The difference Fourier plot, however, showed a residual peak of $9\,e/Å^3$ at the origin. We subsequently occupied the 1*a* site with a further rhodium atom with a free occupancy parameter. The refinement converged readily and the refined composition is in good agreement with the EDX data (see above).

Refinement of the correct absolute structure was ensured through refinement of the Flack parameter (14,15). ZrRhGa has the opposite absolute structure when compared with HfRhGa. In the case of these gallides, there is a large anomalous dispersion effect from the rhodium atoms.

TABLE 2
Atomic Coordinates and Anisotropic Displacement Parameters (pm^2) for ZrRhGa, HfRhGa, and $ZrRh_{0.710(4)}In$

Atom	Wyckoff site	x	y	z	U_{11}	U_{22}	U_{33}	U_{12}	U_{iso}/U_{eq}
ZrRhGa									
Zr	3*f*	0.3952(2)	0	0	77(4)	67(5)	55(6)	34(2)	68(3)
Rh1[a]	2*e*	0	0	0.0573(8)	—	—	—	—	68(4)
Rh2	2*d*	$\frac{1}{3}$	$\frac{2}{3}$	$\frac{1}{2}$	56(3)	U_{11}	83(6)	$1/2U_{22}$	65(3)
Ga	3*g*	0.7296(2)	0	$\frac{1}{2}$	139(5)	47(6)	121(8)	23(3)	112(3)
HfRhGa									
Hf	3*f*	0.60921(8)	0	0	100(2)	87(3)	65(2)	44(1)	85(2)
Rh1[a]	2*e*	0	0	0.9414(8)	—	—	—	—	77(5)
Rh2	2*d*	$\frac{2}{3}$	$\frac{1}{3}$	$\frac{1}{2}$	57(3)	U_{11}	99(6)	$1/2U_{22}$	71(3)
Ga	3*g*	0.2721(3)	0	$\frac{1}{2}$	155(6)	48(7)	113(7)	24(3)	117(3)
$ZrRh_{0.710(4)}In$									
Zr	3*f*	0.5813(2)	0	0	120(4)	165(6)	98(6)	82(3)	123(3)
Rh1[b]	1*a*	0	0	0	—	—	—	—	286(67)
Rh2	2*d*	$\frac{2}{3}$	$\frac{1}{3}$	$\frac{1}{2}$	70(3)	U_{11}	165(8)	$1/2U_{22}$	102(3)
In	3*g*	0.2359(1)	0	$\frac{1}{2}$	84(3)	75(4)	213(5)	37(2)	125(2)

[a] The Rh1 positions of the gallides were refined as split positions with a fixed occupancy of 50%.
[b] The Rh1 position of the indide is occupied only by 12(1)%. U_{eq} is defined as one-third of the trace of the orthogonalized U_{ij} tensor. The anisotropic displacement factor exponent takes the form $-2\pi^2[(ha^*)^2U_{11} + \cdots + 2hka^*b^*U_{12}]$. $U_{23} = U_{13} = 0$.

To give an example, for HfRhGa the weighted residuals were w$R2 = 0.1420$ for the wrong absolute structure as compared to w$R2 = 0.0326$ for the correct one.

As a check for the correct site assignment, all occupancy parameters were refined in a separate series of least-squares cycles along with the displacement parameters. No deviation from full occupancy was observed for both gallides. Only the 1*a* site of the indide showed a partial occupancy. In the final cycles the ideal occupancy parameters were assumed, with the exception of the occupancy parameter of the Rh1 site of the indide. The refinement then readily converged to the residuals listed in Table 1 and the composition was $ZrRh_{0.710(4)}In$ for the crystal investigated. Final difference Fourier syntheses were flat (Table 1). The positional parameters and interatomic distances of the three refinements are listed in Tables 2 and 3. Listings of the observed and calculated structure factors are available.[2]

Crystal Chemistry

The crystal structures of ZrRhGa, HfRhGa, and $ZrRh_{0.710(4)}In$ have been refined from high-quality single-crystal X-ray data. From the c/a ratios (0.467 for ZrRhGa and 0.453 for HfRhGa) one could have expected a superstructure for both gallides. Careful analysis of the crystals by Buerger precession photographs, however, gave no indication for an enlargment of the unit cells. Furthermore, the HfRhGa sample was investigated by electron diffraction and for the ZrRhGa crystal we collected temperature-dependent data sets. Also, these experiments revealed no superstructure reflections.

Refinements of the structures of ZrRhGa and HfRhGa could only be performed with split positions (2*e* 00*z* instead of 1*a* 000) for the Rh1 atoms. The gallium atoms respond to this rhodium dislocation by a slightly larger displacement parameter U_{11}. If a rhodium atom moves off the mirror plane, the gallium atoms forming the trigonal prism around the origin dislocate in the *a* direction. Considering the differently occupied Wyckoff positions, ZrRhGa and HfRhGa are, strictly speaking, not isotypic with ZrNiAl.

At this point, we briefly comment on the course of the lattice parameters of ZrRhGa and HfRhGa. Due to the lanthanoid contraction, the metallic and covalent radii of hafnium are smaller than those of zirconium. Consequently, we observe a smaller cell volume for HfRhGa. However, the course of the *a* and *c* parameters is different. ZrRhGa has the smaller *a* parameter while for HfRhGa the *c* parameter is reduced. This behavior is most likely due to electronic reasons.

A projection of the HfRhGa unit cell is shown in Fig. 1. Both crystallographically different rhodium atoms are located in tri-capped trigonal prisms, i.e., $[Rh1Ga_6Hf_3]$ and $[Rh2Ga_3Hf_6]$. These prisms are condensed via common edges and faces. Together the rhodium and gallium

[2] Details may be obtained from: Fachinformationszentrum Karlsruhe, D-76344 Eggenstein-Leopoldshafen (Germany), by quoting the Registry Nos. CSD-412267 (ZrRhGa), CSD-412268 (HfRhGa), and CSD-412269 ($ZrRh_{0.710(4)}In$).

TABLE 3
Interatomic Distances (pm) Calculated with the Lattice Parameters Taken from X-Ray Powder Data of ZrRhGa, HfRhGa, and $ZrRh_{0.710(4)}In$

		ZrRhGa				HfRhGa				$ZrRh_{0.710(4)}In$	
Zr:	4	Rh2	278.3(1)	Hf:	4	Rh2	277.2(1)	Zr:	4	Rh2	278.7(1)
	2	Rh1	285.7(1)		2	Rh1	283.7(1)		2	In	303.4(1)
	2	Ga	294.2(2)		2	Ga	294.1(2)		1	Rh1	310.6(1)
	4	Ga	303.4(1)		4	Ga	300.1(1)		4	In	317.7(1)
	2	Zr	336.7(2)		2	Hf	328.0(1)		2	Zr	335.8(1)
	4	Zr	383.7(1)		4	Hf	387.2(2)		4	Zr	385.4(1)
Rh1:	1	Rh1	[38.6(5)]	Rh1:	1	Rh1	[38.4(5)]	Rh1:	6	In	242.5(1)
	3	Ga	245.5(2)		3	Ga	244.5(2)		3	Zr	310.6(1)
	3	Ga	270.7(2)		3	Ga	269.1(2)				
	3	Zr	285.7(1)		3	Hf	283.7(1)				
	1	Rh1	298.1(6)		1	Rh1	289.6(5)				
	2	Rh1	336.7(2)		2	Rh1	328.0(1)				
Rh2:	3	Ga	266.1(1)	Rh2:	3	Ga	266.4(2)	Rh2:	6	Zr	278.7(1)
	6	Zr	278.3(1)		6	Hf	277.2(1)		3	In	290.3(1)
Ga:	2	Rh1	245.5(2)	Ga:	2	Rh1	244.5(2)	In:	2	Rh1	242.5(1)
	2	Rh2	266.1(1)		2	Rh2	266.4(2)		2	Rh2	290.3(1)
	2	Rh1	270.7(2)		2	Rh1	269.1(2)		2	In	303.2(1)
	2	Zr	294.2(2)		2	Hf	294.1(2)		2	Zr	306.4(1)
	4	Zr	303.4(1)		4	Hf	300.1(1)		4	Zr	317.1(1)
	2	Ga	336.7(2)		2	Ga	328.0(1)		2	In	335.8(1)
	2	Ga	337.9(3)		2	Ga	341.3(4)				

Note. All distances within the first coordination sphere are listed. Standard deviations are given in parentheses. The short distances within square brackets result from the split position. Only one of these sites can be occupied in an ordered arrangement.

atoms build a three-dimensional [RhGa] network with Rh–Ga distances ranging from 245 to 269 pm. The shorter of these distances compare well with the sum of the metallic single-bond radii of 250 pm (16). The Ga–Ga distances within the triangles of the trigonal prisms are 338 pm in ZrRhGa and 341 pm in HfRhGa, significantly larger than the average Ga–Ga distance (270 pm) in metallic gallium (17). The [RhGa] network is thus mainly governed by strong Rh–Ga interactions.

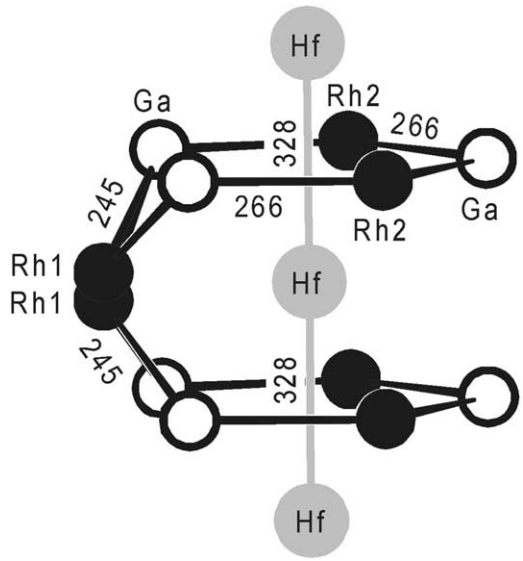

FIG. 2. Distorted pentagonal-prismatic coordination of the hafnium atoms in HfRhGa. Atom designations and relevant interatomic distances (pm) are indicated.

The zirconium (hafnium) atoms are located in distorted pentagonal prismatic channels of the three-dimensional [RhGa] network (Fig. 2). Together, the zirconium (hafnium) atoms form linear chains at Zr–Zr (Hf–Hf) distances of 337 and 328 pm (the *c* lattice parameters), respectively. These distances are only slightly larger than in *hcp* zirconium (321 pm average Zr–Zr distance) and hcp hafnium (316 pm average Hf–Hf distance) (17). We can thus assume also a significant degree of Zr–Zr and Hf–Hf bonding in these gallides. Recently, we analyzed chemical bonding in ZrRhSn (2) and in the indium compound $Ti_3Rh_2In_3$ (8) on the basis of extended Hückel and LMTO electronic structure calculations. For more details we refer to these studies.

In $ZrRh_{0.710(4)}In$, the void at the origin is occupied only by 12(1)% rhodium atoms. To our knowledge, it is the first compound in the Fe_2P structure family where these defects occur. The reason for this behavior is yet unknown. $ZrRh_{0.710(4)}In$ is between $Ti_3Rh_2In_3$ (8) with empty $[In_6]$ trigonal prisms and HfRhGa with a full occupancy. The Rh1–In distances are 243 pm, significantly smaller than the sum of Pauling's single-bond radii (16) of 275 pm for

rhodium and indium. In the various alkaline earth and rare earth metal–rhodium indides, the Rh–In distances cover the large range from 260 to 292 pm (18).

In $Ti_3Rh_2In_3$ (8), the Rh–In distances would be even shorter (231 pm) if the void at the origin would be filled with rhodium atoms. The occupancy of these voids is directly related to the size of the electropositive metal. With the small titanium atoms (metallic radius 146 pm (19)) the voids remain empty, while a small occupancy is observed with zirconium (160 pm metallic radius (19)). With the much larger yttrium atoms (180 pm) full occupancy is observed (20). Based on these results, we expect a small homogeneity range $ZrRh_{0.71\pm x}In$ for the zirconium compound and with hafnium (158 pm metallic radius), we expect the formation of $Hf_3Rh_2In_3$ or $Hf_3Rh_{2+x}In_3$. These investigations are currently in progress.

Finally, we draw back to the $ZrRh_{0.710(4)}In$ structure. The In–In distances within the trigonal prism around the origin are 303 pm within the triangular faces and 336 pm within the rectangular ones. These compare well with the In–In distances in tetragonal indium, where each indium atom has four neighbors at 325 pm and eight ones at 338 pm (17). In comparison with the ZrRhGa and HfRhGa discussed above, In–In bonding plays a more dominant role in $ZrRh_{0.710(4)}In$ than Ga–Ga bonding in the two gallides. The Zr–Zr distances in ZrRhGa (337 pm) and $ZrRh_{0.710(4)}In$ (336 pm), however, are similar.

ACKNOWLEDGMENTS

We are grateful to Dipl.-Ing. U. Ch. Rodewald and Dr. H. Piotrowski for the intensity data collections, to J. Göcke for the EDX analyses, and to Prof. Dr. A. Putnis for taking the electron diffraction patterns. This work was financially supported by the Fonds der Chemischen Industrie and the Deutsche Forschungsgemeinschaft.

REFERENCES

1. M. F. Zumdick and R. Pöttgen, *Z. Kristallogr.* **214,** 90 (1999).
2. M. F. Zumdick, R.-D. Hoffmann, and R. Pöttgen, *Z. Naturforsch.* **54b,** 45 (1999).
3. P. I. Krypyakevich, V. Ya. Markiv, and E. V. Melnyk, *Dopov. Akad. Nauk. Ukr. RSR, Ser. A* 750 (1967).
4. A. E. Dwight, M. H. Mueller, R. A. Conner Jr., J. W. Downey, and H. Knott, *Trans. Met. Soc. AIME* **242,** 2075 (1968).
5. R. Mishra, R. Pöttgen, R.-D. Hoffmann, H. Trill, B. D. Mosel, H. Piotrowski, and M. F. Zumdick, *Z. Naturforsch.* **56b,** 589 (2001).
6. D. Kußmann, R. Pöttgen, B. Künnen, G. Kotzyba, R. Müllmann, and B. D. Mosel, *Z. Kristallogr.* **213,** 356 (1998).
7. R. Pöttgen, A. Lang, R.-D. Hoffmann, B. Künnen, G. Kotzyba, R. Müllmann, B. D. Mosel, and C. Rosenhahn, *Z. Kristallogr.* **214,** 143 (1999).
8. M. F. Zumdick, G. A. Landrum, R. Dronskowski, R.-D. Hoffmann, and R. Pöttgen, *J. Solid State Chem.* **150,** 19 (2000).
9. A. E. Dwight, *J. Less-Common Met.* **34,** 279 (1974).
10. R. Pöttgen, Th. Gulden, and A. Simon, *GIT-Laborfachzeitschrift* **43,** 133 (1999).
11. K. Yvon, W. Jeitschko, and E. Parthé, *J. Appl. Crystallogr.* **10,** 73 (1977).
12. G. M. Sheldrick, "Shelxs-97, Program for the Solution of Crystal Structures," University of Göttingen, 1997.
13. G. M. Sheldrick, "Shelxl-97, Program for Crystal Structure Refinement," University of Göttingen, 1997.
14. H. D. Flack and G. Bernadinelli, *Acta Crystallogr. A* **55,** 908 (1999).
15. H. D. Flack and G. Bernadinelli, *J. Appl. Crystallogr.* **33,** 1143 (2000).
16. L. Pauling, "The Nature of the Chemical Bond and The Structures of Molecules and Crystals." Cornell University Press, Ithaca, NY, 1960.
17. J. Donohue, "The Structures of the Elements." Wiley, New York, 1974.
18. R.-D. Hoffmann, H. Huppertz, and R. Pöttgen, *Solid State Sciences* **4,** 103 (2002).
19. E. Teatum, K. Gschneidner Jr., and J. Waber, "Rep. LA - 2345." US Department of Commerce, Washington, DC, 1960.
20. R. Ferro, R. Marazza, and G. Rambaldi, *Z. Anorg. Allg. Chem.* **409,** 219, 1974.